Science of the Total Environment 1005 (2025) 180878

Contents lists available at ScienceDirect

Science of the Total Environment

journal homepage: www.elsevier.com/locate/scitotenv

Cellular insights into reactive oxidative species (ROS) and bacterial stress responses induced by antimicrobial blue light (aBL) for inactivating antibiotic resistant bacteria (ARB) in wastewater

Xiaoyu Cong [a], Jasna Hillert [a], Peter Krolla [a], Thomas Schwartz [a,*]

[a] Karlsruhe Institute of Technology (KIT), Institute of Functional Interfaces (IFG), Hermann von Helmholtz Platz 1, 76344, Eggenstein-Leopoldshafen, Germany

HIGHLIGHTS

- aBL irradiation results in different cellular responses in antibiotic resistant bacteria: inactivation or viable but not culturable.
- Scavenger experiments underline the role of ROS during the aBL mediated inactivation of wastewater bacteria
- Specific ROS ($^1O_2$ and H_2O_2) were identified as key contributors to bacterial inactivation under aBL and much stronger aBL in combination with photosensitizers.
- Oxidative stress responsive genes are up-regulated, whereas membrane integrity linked gene are reduced in expression during aBL irradiation.

GRAPHICAL ABSTRACT

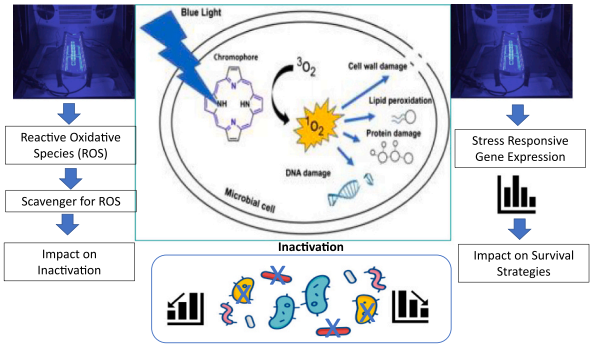

ARTICLE INFO

Keywords:
antimicrobial blue light (aBL)
antibiotic resistances
reactive oxidative species (ROS)
oxidative stress response
wastewater disinfection effectiveness

ABSTRACT

The global threat of antimicrobial resistance (AMR), largely driven by the long-term misuse of antibiotics, highlights the urgent need for decentralized disinfection methods. Our previous study confirmed the effectiveness of antimicrobial blue light (aBL) against AMR. However, the underlying cellular mechanisms remained unexplored. However, the underlying cellular mechanisms remained unexplored. Here, we address this gap by combining selective ROS scavenger assays with transcriptional profiling of oxidative stress responsive genes, thereby providing mechanistic insights into the inactivation of facultative pathogenic bacteria (FPB) and antibiotic resistance genes (ARGs) under aBL treatments.

A multidrug-resistant *Pseudomonas aeruginosa* and *van*A-positive *Enterococcus faecium* reference strain were treated with aBL alone and aBL combined with TMPyP. Discrepancies between cultivation and quantitative PCR (qPCR) results revealed the presence of viable but non-culturable (VBNC) cells in case of *P. aeruginosa*, underscoring the necessity of combining both approaches to reliably assess aBL inactivation. Among all treatments, aBL combined with sub-lethal TMPyP concentrations of (10^{-6} M) proved the most effective, with reactive oxidative species (ROS) analysis identifying singlet oxygen ($^1O_2$) and hydrogen peroxide (H_2O_2) as the primary reactive species responsible for bacterial inactivation. Stress responsive gene expression analysis under three treatment conditions (aBL alone, aBL + H_2O_2 (1 mM), aBL + TMPyP (10^{-6} M)) showed an upregulation of *sod*A (>2.4-fold), *rec*A (>2.5-fold), *oxy*R (>3.1-fold), and *tol*C (>4.2-fold), particularly under aBL + TMPyP treatment,

* Corresponding author.
E-mail address: thomas.schwartz@kit.edu (T. Schwartz).

https://doi.org/10.1016/j.scitotenv.2025.180878
Received 19 August 2025; Received in revised form 2 October 2025; Accepted 1 November 2025
Available online 7 November 2025
0048-9697/© 2025 The Authors. Published by Elsevier B.V. This is an open access article under the CC BY license (http://creativecommons.org/licenses/by/4.0/).

indicating strong oxidative stress responses. In contrast, the downregulation of *ompF* suggests a membrane-protective mechanism aimed at reducing permeability to harmful substances. Unlike previous aBL studies, our work links ROS specificity with bacterial stress adaptation, supporting the potential of aBL as a scalable and mechanistically understood strategy for decentralized wastewater disinfection at AMR hotspots.

1. Introduction

Antibiotics are recognized as a new type of environmental pollutants because of their persistence and potential ecotoxicological effects (Shao et al., 2018). The selective pressure from long-term antibiotic use drives the evolution of resistant bacterial variants (Amarasiri et al., 2020; Li and Zhang, 2022), leading to AMR, which is estimated to lead to 10 million deaths annually globally by 2050 (Tang et al., 2023; O'Neill, 2016). Antibiotic resistant bacteria (ARB) and ARGs are gaining gradual acceptance as environmental pollutants, raising considerable public health concerns (Ding et al., 2023; Ondon et al., 2021) and are found to contribute to hospital-acquired infections (Li et al., 2023).

Conventional wastewater treatment strategies generally cannot effectively remove ARB/ARGs and this urges the development of novel and efficient remediation measures (Mandal, 2024; Wang and Chen, 2022). Of the possibilities currently under examination, the advanced oxidation processes (AOPs) have been extensively studied for the elimination of ARB and ARGs (Alexander et al., 2016; Ferro et al., 2017), but their broader application is hindered by high cost, high energy demand, and the formation of potential harmful by-products (Han et al., 2024). aBL has emerged as a promising, environmentally sustainable alternative to conventional UV-based approaches. Compared with medium-pressure UV lamps, LED-based aBL systems are substantially more efficient in the 405 nm range (Martín-Sómer et al., 2023), roughly 20 times higher radiation output for the same energy input, while avoiding undesired side reactions. Their mercury-free, modular design further enables safe, scalable deployment at critical hotspots in wastewater treatment and facilitates retrofitting of legacy infrastructure. Given that effluents can still contain trace pollutants and multi-resistant bacteria, extending hygienisation with LED-based aBL offers an environmentally sustainable option to safeguard public health and the environment (Mandal, 2024).

Mechanistically, aBL acts by stimulating native bacterial chromophores irradiating bluelight with the help of LED lamp technology. In subsequence, the formed ROS include hydroxyl radicals ($OH^{\bullet}$), superoxide anions ($O_2^{\bullet-}$), $^1O_2$, and H_2O_2 contribute to the bactericidal effect (Feuerstein et al., 2005; Wang et al., 2019). These ROS cause oxidative damages to DNAs, proteins, and membranes, which ultimately result in microorganism death. Our previous study demonstrated the feasibility of aBL in a continuous flow reactor, achieving substantial reductions of 4 FPB, 10 ARGs, as well as 16S rRNA and *Intl*1 genes (Cong et al., 2025). While these findings verified the feasibility of aBL in practice, the specific cellular mechanisms of action under wastewater conditions remain unclear.

ROS are generated under aBL through two distinct photochemical pathways: One, the type I mechanism, involves electron transfer to produce H_2O_2, $OH^{\bullet}$, and $O_2^{\bullet-}$. In the mechanism type II energy transfer to molecular oxygen results mainly in $^1O_2$ (Dąbrowski, 2017; Baptista et al., 2021). Exogenous photosensitizers (PS) such as porphyrins can be added to increase ROS production and consequently aBL efficiency (Cong et al., 2023; Bulit et al., 2014). Our own studies (Cong et al., 2023, 2025) have demonstrated that the application of photosensitizers and oxidative agent (TMPyP or H_2O_2) in aBL irradiation could greatly improve ARGs and FPB elimination by raising hypothesized oxidative stress.

Although the bactericidal activity of aBL is widely attributed to ROS, the specific contributions of individual ROS species during disinfection in wastewater matrices remain unclear. To address this gap, we applied selective scavengers to determine the relative contributions of individual ROS. The effect of each ROS was further assessed by qPCR with respect to a gene copy number determination of *erm*B, *sec*E (specific for *A. baumannii*), bla_{TEM}, 16S rRNA genes. Since VBNC cells escape detection by conventional cultivation methods (Colwell, 2000), culture-independent molecular tools are essential. In this study, living/dead differentiation combined with qPCR provided a more comprehensive and reliable assessment of ARB and ARG persistence under aBL treatment.

Under aerobic conditions, molecular oxygen freely diffuses across biological membranes, participating in intracellular ROS formation. To survive in such oxidative environments, bacteria have evolved sophisticated stress response systems. While ROS are central to microbial inactivation, they can also contribute to the development of antibiotic resistance by inducing DNA damage and mutagenesis during DNA repair mediated by *rec*A gene activation (Taylor et al., 2024; Qi et al., 2023). In response to such oxidative stress, bacteria have constitutive expression of an array of antioxidant enzymes that scavenge ROS and repair oxidative damage. Moreover, the synthesis of most of these enzymes is induced as intracellular ROS resulting in a dynamic and inducible protection system. OxyR and SoxRS are major regulatory proteins that are activated by oxidants to promote the up-regulation of genes associated with detoxification and repair in response to H_2O_2 exposure (Chiang and Schellhorn, 2012; Choudhary et al., 2024). On reversible oxidation, the oxidized OxyR positively interacts with the RNA polymerase and thereby increases transcription of its target genes (Bang et al., 2016). The *sod*A gene, encoding superoxide dismutase (SOD), catalyzes the disproportionation of $O_2^{\bullet-}$ to H_2O_2 and oxygen, and represents the main protection system against oxidative stress (Wang et al., 2024). *rec*A is a key regulator gene central to the SOS response, promoting DNA repair during oxidative damage (Sanchez-Alberola et al., 2012). Notably, activation of *rec*A not only promotes DNA repair but also facilitates horizontal gene transfer, thereby accelerating the evolution of resistance. Membrane-associated stress-response genes such as *tol*C (efflux pump) and *omp*F (porin) help bacteria adapt to redox stress and maintain membrane integrity (Sorn et al., 2023; Wang et al., 2024).

In our previous study, we demonstrated the feasibility of aBL for the removal of 4 FPB, 10 ARGs, as well as 16S rRNA and *Intl*1 genes, confirming its practical applicability in wastewater matrices. Here, we report on the inactivation of two relevant facultative pathogenic bacterial strains both carrying ARGs with clinical relevance, namely *P. aeruginosa* PA49 and *E. faecium* B7641, after different aBL treatment. The study uses both culture-based (colony forming unit (CFU)) and qPCR methods to compare how various analytical methods can affect the interpretation of treatment efficacy. Furthermore, the expression levels of genes involving the bacterial responses to stress under oxidative environments induced by aBL have been determined by reverse transcription quantitative PCR (RT-qPCR). The levels of expression of oxidative stress responsive genes (*oxy*R, *sod*A, *rec*A, *omp*F, and *tol*C) monitored provided an insight into the mechanism of bacterial adaptation and survival. Several studies have documented the evolution of aBL resistance. We therefore see an urgent need to understand the cellular mechanisms of aBL in the wastewater matrix (Kruszewska-Naczk et al., 2024; Rapacka-Zdonczyk et al., 2021). By integrating ROS scavenger assays with RT-qPCR analysis of oxidative stress responsive genes, this study for the first time elucidates the cellular mechanisms of aBL disinfection within a complex wastewater matrix, providing novel insights into bacterial adaptation and highlighting the potential of aBL as a sustainable light-based technology for decentralized wastewater treatment. In Fig. 1 our analytical strategy is presented to get a more

comprehensive understanding of cellular activities of some facultative pathogenic wastewater bacteria to aBL/photosensitizer mediated treatments. The final goal is the development of an optimized strategy to inactivate hygienically relevant microorganisms in wastewater hotspots.

2. Methods

2.1. Strains and culture conditions

The bacterial strains used in the aBL assays were *P. aeruginosa* PA49 which is a multi-resistant wastewater isolate (Berditsch et al., 2015) and *E. faecium* B7641 which is a strain of the German collection of microorganisms and contains the *van*A Vancomycin resistance gene (Patel et al., 1997). Primer sequences, amplicon sizes, qPCR conditions, and control strains are provided in Table S1. *P. aeruginosa* and *E. faecium* cultures were performed by transferring 1.5 mL of an overnight culture to 13.5 mL of LB medium (Luria-Bertani, Sigma-Aldrich, Darmstadt, Germany) and incubated at 37 °C with shaking (56 rpm) (CERTOMAT H, Labexchange, Burladingen, Germany). The growth of bacteria was assessed by measuring the optical density at 600 nm (OD_{600}) to be 0.8 with a Hitachi photometer (Hitachi High-Tech Corporation, Tokyo, Japan), which indicates bacterial exponential growth. Following a seven-step serial dilution of the bacterial suspension at a ratio of 1:10 using phosphate-buffered saline (PBS), five drops of each dilution, each with a volume of 10 μL, were plated onto agar media. Colony counts were determined after incubating using the drop plate method (Herigstad et al., 2001). The CFU were then calculated by averaging the number of colonies across the five drops and converting the result to CFU/mL according to the respective dilution factor.

2.2. Chemical reagents and ROS quantification in scavenger studies

Chemical scavengers were applied to explore the roles of individual ROS in aBL. Based on their established specificity in biological ROS studies, 10 mM L-histidine (ITW Reagents) for $^1O_2$ (Méndez-Hurtado et al., 2012), 10 mM Tiron (Thermo Scientific) for $O_2^{\bullet-}$ (Taiwo, 2008), 10 mM *tert*-butanol (VWR International GmbH) for $OH^\bullet$ (Piechowski et al., 1992), and 10 mM Na_2SO_3 (Sigma-Aldrich) for H_2O_2 (Wang et al., 2013) were added to water samples separately for quenching the respective ROS. Preliminary dose–response pre-experiments (1, 5, and 10 mM) confirmed that 10 mM provided consistent scavenging activity without affecting bacterial viability in dark controls, as shown in Fig. S1. Parallel control samples without scavenger treatment were prepared for comparison. The degradation rate for each aBL-related treatment, both with and without additional scavengers, was determined by calculating the rate constant based on a pseudo-first-order kinetic model, as described by the following equation (Eq. 1):

$$\ln\left(\frac{C_0}{C_t}\right) = kt \tag{1}$$

In this equation, C (copies/100 mL) represents the gene copy number of the 16S rRNA gene, t (min) is the reaction time, and k (min^{-1}) is the pseudo-first-order rate constant. Additionally, the contribution rate of ROS, denoted as RC, was estimated using the following equation:

$$RC \bullet OH^\bullet = \frac{k_{OH^\bullet}}{k_{app}} \approx \frac{k_{app} - k_{tert-butanol}}{k_{app}} \tag{2}$$

$$RC \bullet O_2^{\bullet-} = \frac{kO_2^{\bullet-}}{k_{app}} \approx \frac{k_{app} - k_{Tiron}}{k_{app}} \tag{3}$$

$$RC \bullet {}^1O_2 = \frac{k_{^1O_2}}{k_{app}} \approx \frac{k_{app} - k_{L-histidine}}{k_{app}} \tag{4}$$

$$RC \bullet H_2O_2 = \frac{k_{H_2O_2}}{k_{app}} \approx \frac{k_{app} - k_{Na2SO3}}{k_{app}} \tag{5}$$

In these equations, k_{app} is the apparent rate constant for 16S rRNA gene degradation in the control group (without scavenger), while $k_{tert\text{-}butanol}$, k_{Tiron}, $k_{L\text{-}histidine}$, and k_{Na2SO3} represent the rate constants in the presence of specific ROS scavengers targeting $OH^\bullet$, $O_2^{\bullet-}$, $^1O_2$, and H_2O_2, respectively.

2.3. Sampling and experimental setup

2.3.1. Experimental setup for CFU and qPCR comparison

To compare culture-based and molecular quantification methods, bacterial suspensions from the reference strains *P. aeruginosa* PA49 and *E. faecium* B7641 were prepared and processed as follows: From the 11 mL bacterial suspension, 5.0 mL were aliquoted into 2.0 mL reaction

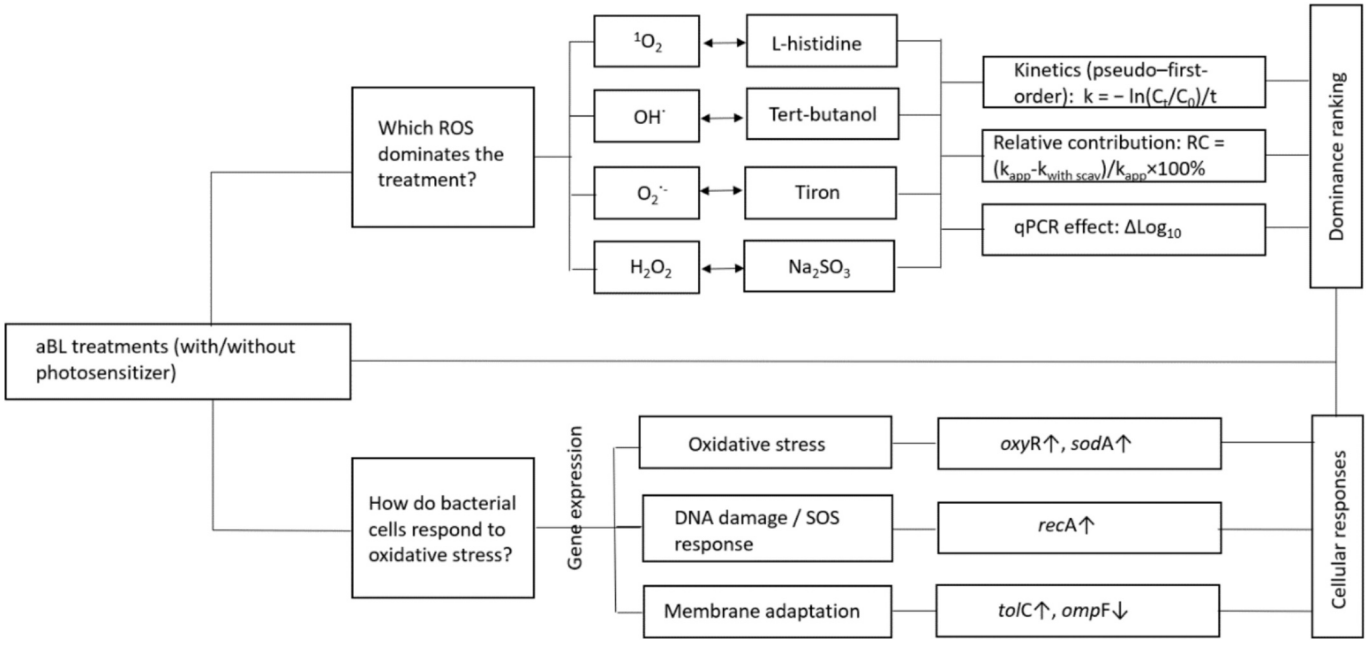

Fig. 1. Mechanistic workflow used to infer ROS dominance and cellular responses under aBL with/without photosensitizer.

tubes and centrifuged (BIOFUGE pico, Heraeus, Waltham, USA). The supernatant was discarded and the pellets were resuspended in 50 μL of PBS. The suspensions from the three reaction tubes were combined in a single 2.0 mL tube and stored at −18 °C. This constituted the initial sample (t_o) for subsequent DNA extraction. Additionally, 200 μL were transferred into a 1.5 mL tube for the t_o dilution series and cultivation. The same procedure was repeated following aBL treatment, representing the irradiated samples.

For aBL irradiation, 5.2 mL of bacterial suspension were placed in sterile 10 mL glass vials with sterilized magnetic stir bars (Ø 2 mm × 5 mm). In selected samples, TMPyP was added to a final concentration of 10^{-6} M, shown to effectively reduce ARB in aBL applications (Cong et al., 2023). The photosensitizer in use, TMPYP was obtained from Sigma-Aldrich (Darmstadt, Germany). 5,10,15,20-Tetrakis(1-methyl-4-pyridinio)-porphyrin tetra (p-toluenesulfonate) (TMPyP) is a well-known PS used for aBL (Chaves et al., 2017). TMPyP has a planar tetracationic structure of porphyrin ring system (Fig. S2), which makes it to have a strong absorbance in the visible light and especially in Soret band (~400 nm), which is proper for photodynamic activation. A stock solution of TMPyP at 10^{-3} M is employed. 1×10^{-6} M, the more diluted sample, was taken for experimental purposes as well. Concentrations of TMPyP are selected based on empirical work that has shown them to be most effective in combatting antibiotic resistance (Cong et al., 2023). These samples were incubated in the dark for 30 min, and subsequent handling was performed under light-protected conditions to prevent unintended PS activation.

The static aBL photoreactor used in this experiment (Fig. S3) differed from the system applied for scavenger studies and oxidative stress gene expression analysis. It consisted of six LED lamps (L XS series, S/N 0281; Opsytec Dr. Gröbel GmbH, Ettlingen, Germany), each emitting at 420 nm with a total energy dose of 245 W/m^2 and 98.4 % radiation intensity. Glass vials were placed on a magnetic stirrer (2Mag) mounted on a height-adjustable platform (Swiss Boy), both secured with adhesive foil, maintaining a 15.5 cm distance from the LEDs. The entire setup was housed in a temperature-controlled incubator (Memmert ICP 600) at 20 °C to prevent heat-induced effects. Irradiation conditions included: 2 h aBL, 4 h aBL, and 2 h aBL + TMPyP (10^{-6} M), each with $n = 3$ replicates.

2.3.2. Wastewater samples collection and experimental setup for scavenger studies and gene expression

To evaluate the role of ROS and bacterial oxidative stress responses under aBL treatment, wastewater samples were collected from the local wastewater treatment plant (WWTP) influent located on the campus of the Karlsruhe Institute of Technology (KIT) in Karlsruhe, Germany. This facility primarily receives wastewater from scientific research institutes and serves a population of approximately 3300 individuals, including international researchers and students during the academic week. The WWTP processes around 450 m^3 of wastewater daily using a combination of conventional physical and biological treatment methods. Influent samples from the WWTP were collected for further analysis.

The scavenger study primarily focused on aBL alone and aBL combined with TMPyP. Both scavenger-containing and control samples (without scavengers) were transferred into sterile 20-mL glass vials, each containing a sterilized magnetic stir bar (Ø 2 mm × 5 mm) and subjected to aBL treatment in a static photoreactor setup. For each individual scavenger evaluated under both treatment conditions (aBL alone and aBL combined with TMPyP), three independent trials ($n = 3$) were conducted for subsequent molecular analysis. Illumination was provided by four SolarStinger SunStrip DeepBlue LED bars (Econlux, Germany), each incorporating chips at 400, 420, 440, and 460 nm to deliver a broad-spectrum blue light source (Fig. S4). Further technical details are available in our previous study (Cong et al., 2023).

However, for the gene expression analysis of oxidative stress–responsive genes, all three treatment regimens were included: aBL alone, aBL + TMPyP (10^{-6} M), and aBL + H_2O_2 (1 mM). Oxidative agent H_2O_2 was tested at a final concentration of 1 mM and combined with aBL irradiation for its synergistic effects, as previous studies have also reported enhanced disinfection efficiency when aBL is used together with H_2O_2 (Ngo et al., 2023). The selected dose is within the reported range of ideal concentrations for ROS production without self-scavenging of OH$^\bullet$ (Truong et al., 2020). Control experiments showed that neither TMPyP (1×10^{-6} M) nor H_2O_2 (1 mM) were able to kill the bacteria in the dark without aBL irradiation. Enhanced bacterial inactivation was observed only when these agents were combined with blue light irradiation.

Scavenger assays were performed in triplicate (n = 3), while gene expression experiments were conducted in four independent biological replicates ($n = 4$). For both scavenger analysis and oxidative stress gene expression studies, a static aBL photoreactor (Fig. S4) was used, consistent with the setup previously applied by Cong et al. (2023). Following aBL treatment, 18 mL of sample, whether from the scavenger or gene expression experiments, was passed through a 47 mm, 0.2 μm polycarbonate membrane (Whatman Nucleopore Track-Etched, Sigma-Aldrich, Munich). Following filtration, membranes were treated with 20 μM propidium monoazide (PMA) to differentiate live from dead bacteria. PMA selectively penetrates cells with compromised membranes and binds nucleic acids, thereby preventing amplification during qPCR. Samples were incubated in the dark for 10 min to avoid photodegradation, followed by photo-activation with the PhAST Blue system (GenIUL, Barcelona, Spain) at maximum intensity for 15 min to cross-link PMA to DNA (Cong et al., 2023, 2025). DNA extracted from these filters was used for qPCR in scavenger analysis, and RNA was isolated for gene expression analysis via RT-qPCR.

2.3.3. DNA extraction for qPCR analysis

DNA was extracted using the FastDNA™ Spin Kit for Soil (MP Biomedicals, Santa Ana, USA) in combination with the FASTPREP® homogenization system (MP Biomedicals, Santa Ana, USA). For mechanical cell disruption, the filtered biomass retained on the membranes was transferred into Lysing Matrix E tubes and processed according to the manufacturer's protocol. Proteins were removed by centrifugation and precipitation, and DNA was subsequently purified via binding to a silica matrix. The concentration of the extracted DNA was measured using both a NanoDrop spectrophotometer (ND-1000, PEQLAB Biotechnologie GmbH, Germany) and the Quant-iT™ PicoGreen® dsDNA Assay Kit (Thermo Fisher Scientific, Nidderau, Germany).

qPCR assays using SYBR Green were performed with a Bio-Rad CFX96 Touch™ Deep Well Real-Time PCR Detection System (Bio-Rad, Munich, Germany), and data analysis was conducted using the Bio-Rad CFX Manager Software. Each reaction was carried out in a total volume of 20 μL, consisting of 10 μL Maxima SYBR Green/ROX qPCR Master Mix (2×) (Thermo Scientific, Nidderau, Germany), 7.4 μL nuclease-free water (Ambion, Life Technologies, Karlsbad, Germany), 0.8 μL forward primer (10 μM), 0.8 μL reverse primer (10 μM), and 1 μL of template DNA. Thermal cycling conditions included an initial denaturation step at 95 °C for 10 min, followed by 40 amplification cycles of 15 s at 95 °C and 60 s at 60 °C. Melting curve analysis was performed at the end of each run to verify amplification specificity. In this study, four genetic targets were analyzed to assess bacterial abundance and antibiotic resistance: *secE* (a taxonomic marker gene specific for *Acinetobacter baumannii*), *ermB* (a macrolide resistance gene), 16S rRNA gene (a universal marker for eubacterial abundance), and bla_{TEM} (a β-lactamase gene associated with resistance to penicillins). Primer sequences and related details are provided in Table S2. DNA extraction has also been applied by KITs lab in related wastewater resistance studies (e.g., Hembach et al., 2019).

2.3.4. RNA extraction and RT-qPCR analysis

After the filtration steps, the filters were directly transferred into Lysing Matrix E Tubes (MP™ Biomedicals, USA) and 700 μL of RLT Buffer (QIAGEN, Netherlands) was added. The samples were

homogenized for 40 s using a Fast-Prep R24 (MP™ Biomedicals, USA) and then vortexed for 15 s. The upper aqueous phase was carefully transferred to a new tube, mixed with 700 μL of 70 % ethanol (prepared from absolute ethanol, VWR™ Chemicals, USA), and loaded onto a RNeasy Mini Spin Column. The column was centrifuged at 11,000 rpm for 15 s, and the flow-through was discarded. Next, 350 μL of RW1 buffer was added to the column followed by centrifugation. To remove contaminating DNA, a digestion solution comprising 10 μL of DNase I stock and 70 μL of RDD buffer was applied directly to the column and incubated at room temperature for 15 min. Following incubation, 350 μL of RW1 buffer was added to the column. The column was then washed twice with 500 μL of RPE buffer, with centrifugation after each wash to discard the flow-through. Finally, the column was transferred to a new 1.5 mL collection tube, and 50 μL of RNase-free water was added. After centrifugation at 11,000 rpm for 1 min, the RNA was eluted and collected. RNA concentration was determined using a NanoDrop 1000 Spectrophotometer (peqlab Biotechnologie GmbH, Germany), and the samples were used immediately for cDNA synthesis.

cDNA synthesis was performed using the SuperScript™ IV kit (Thermo Fisher Scientific, USA). For each sample, duplicate reactions were prepared. Thermal cycling was conducted on a C1000 Touch™ Thermal Cycler (Bio-Rad Laboratories, USA). For the annealing step, 1 μL of random hexamer primer, 1 μL of 10 mM dNTPs, and 50 ng of RNA template were combined, and nuclease-free water was added to bring the total volume to 13 μL. The mixtures were vortexed, briefly centrifuged, heated to 65 °C for 5 min, and then cooled to 2 °C for 2 min. For the elongation reaction, 4 μL of 5× SSIV buffer, 1 μL of 100 mM DTT, 1 μL of RNase inhibitor, and 1 μL of SuperScript IV polymerase were added to each reaction. After mixing and a brief centrifugation, the reactions were incubated at 50 °C for 10 min, followed by 80 °C for 10 min. Subsequently, 1 μL of RNase H was added, and the reactions were incubated at 37 °C for 20 min to remove residual RNA. The concentration of cDNA was determined using a NanoDrop 1000 Spectrophotometer (peqlab Biotechnologie GmbH, Germany), and the samples were stored at −20 °C. Additionally, quantitative PCR was performed on all cDNA samples (with the sequence described in Table S2) using bacterial primers. Reactions were performed in volumes of 20 μL containing 10 μL Maxima SYBR Green/ROX qPCR Master Mix (2×) (Thermo Scientific Nidderau, Germany), 7.4 μL nuclease-free water (Ambion, Life technologies, Karlsbad, Germany), 0.8 μL primer forward (10 μM), 0.8 μL primer reverse (10 μM) and 1 μL template DNA. In the denaturation phase, double-stranded DNA was converted into single strands by heating at a high temperature (about 95 °C) for 10 min. This was followed by 40 cycles of 15 s at 95 °C and 60 s at 60 °C. The melting curves were recorded by increasing the temperature from 60 °C to 95 °C (1 °C every 10 s) to assess the specificity of the application. RT-qPCR assays were conducted following the MIQE guidelines for qPCR experiments (Bustin et al., 2009). 16s rRNA was used as a reference gene to which the gene expression values were normalized (Smith and Osborn, 2009), and gene expression levels of stress-response genes were determined using the $2^{-\Delta\Delta Ct}$ method (Pfaffl, 2001; Livak and Schmittgen, 2001), with expression normalized to a housekeeping gene and relative to a control condition. Additionally, the standard curve of all oxidative stress response genes is provided in the supplementary information (Table S4) and the corresponding primer details are listed in Table S2.

2.4. Statistical analysis

Gene expression data were analyzed in Graphpad Prism 10 (Graphpad software) using the two-tailed Mann-Whitney *U* test. Results with $p < 0.05$ were considered statistically significant, while $p < 0.10$ were regarded as trend-level and interpreted with caution (Schacksen et al., 2025). Results with $p < 0.1$ were highlighted in bold in Table 2. Significant values are highlighted in bold in Table 2. Scavenger assay data were compared by one-way ANOVA followed by Tukey's multiple comparison tests to evaluate differences between the control, aBL alone, and aBL combined with TMPyP or H_2O_2. The resulting *p*-values were used to determine statistical significance, which is indicated in the figures as follows: not significant (ns), $p \leq 0.0001$(****), $p \leq 0.001$ (***).

3. Results and discussion

3.1. Reduction effectiveness of aBL irradiation determined by cultivation and qPCR

The antimicrobial efficacy of aBL treatment was assessed by survival of the reference strains *P. aeruginosa* PA49 and *E. faecium* B7641 using culture based (CFU) and molecular methods (qPCR). The initial CFU counts of untreated cultures were 6.8×10^8 for *P. aeruginosa* and 1.7×10^7 CFU/mL for *E. faecium*. The corresponding error bars are shown in Fig. 2.

Both strains showed a decrease in CFU/mL after aBL treatment, as depicted in Fig. 2. In *P. aeruginosa*, 4.6 $\log_{10}$ unit reduction was obtained at 2 h after aBL (2.2×10^3 CFU mL^{-1}). Significantly, the CFU were not detected (n.d.) for both 4 h aBL and 2 h aBL + TMPyP treatments, with an at least 6.5 $\log_{10}$ units reduction. *E. faecium*, on the other hand, was reduced below $\log_{10}$ 4 at 2 h aBL and below $\log_{10}$ 5 at 4 h aBL. Only for the combined treatment (2 h aBL + TMPyP) the CFU were not detected ($\geq$6 $\log_{10}$ unit reduction).

Overall, the results demonstrate that *P. aeruginosa* can be inactivated more effectively by aBL than *E. faecium* as judged by cultivation results. Molecular analyses, however, allowed examination of this discrepancy in susceptibility further. The $\log_{10}$ unit reductions (measured by qPCR, Table 1) in cell equivalents/100 mL are presented in comparison to the initial numbers at t_0. It is worth noting that *in P. aeruginosa*, while the taxonomic marker gene (*ecfX*) and the resistance gene (bla_{VIM}) themselves were not completely depleted by aBL treatment, combined with TMPyP, respectively. Such a limited efficacy at the DNA level despite pronounced CFU loss could also explain that the highest observed drop was 1.17 $\log_{10}$ for *ecfX* and 1.42 $\log_{10}$ for bla_{VIM} for aBL plus TMPyP. These results are consistent with the previous study of Cong et al. (2025), indicating that culturability may be lost in *P. aeruginosa* under oxidative stress, while DNA is mostly preserved. In contrast, *E. faecium* showed only minimal gene copy number reduction after aBL exposure alone. Notably, at 2 h, we observed a small rise in cell equivalents. This transient increase does not indicate growth. One hypothesis is rapid repair of sublethal oxidative lesions caused by aBL. This repair could resuscitate VBNC cells and restore culturability, which raises CFU relative to t0 while qPCR targets remain stable. A second hypothesis is an analytical effect in qPCR. Inactivation treatments can disrupt envelopes and matrices, release intracellular DNA, and reduce PCR inhibition. These changes improve target recovery and lower Cq values, so gene copies per milliliter can appear to increase even as cellular activity declines. However, when aBL was combined with TMPyP, a marked decrease was observed, specifically, 5.61 $\log_{10}$ and 7.14 $\log_{10}$ unit reductions in the enterococci specific 23S rRNA gene and vancomycin *van*A resistance gene in *E. faecium*, respectively. These results demonstrate the enhanced efficacy of aBL treatment when photoactivation is intensified by TMPyP and highlight *E. faecium*'s greater vulnerability to DNA-targeted oxidative damage under these conditions.

This discrepancy between CFU and qPCR is particularly pronounced in *P. aeruginosa*. While culture results indicate high susceptibility to aBL, qPCR suggests that the DNA of these cells remains largely intact. This observation is indicative of a "VBNC" state in which the bacteria are metabolically active but not culturable in the synthetic nutrient media. Consistent with this, DNA integrity in aBL-exposed *P. aeruginosa* was not affected and gene copy numbers were constant. For *E. faecium*, the correlation between CFU loss and qPCR data was better, especially upon aBL + TMPyP treatment. However, a minor discrepancy still suggests the presence of VBNC cells or sub-lethally damaged DNA.

These observations underscore the need of combining culture-based and molecular techniques when assessing antimicrobial interventions.

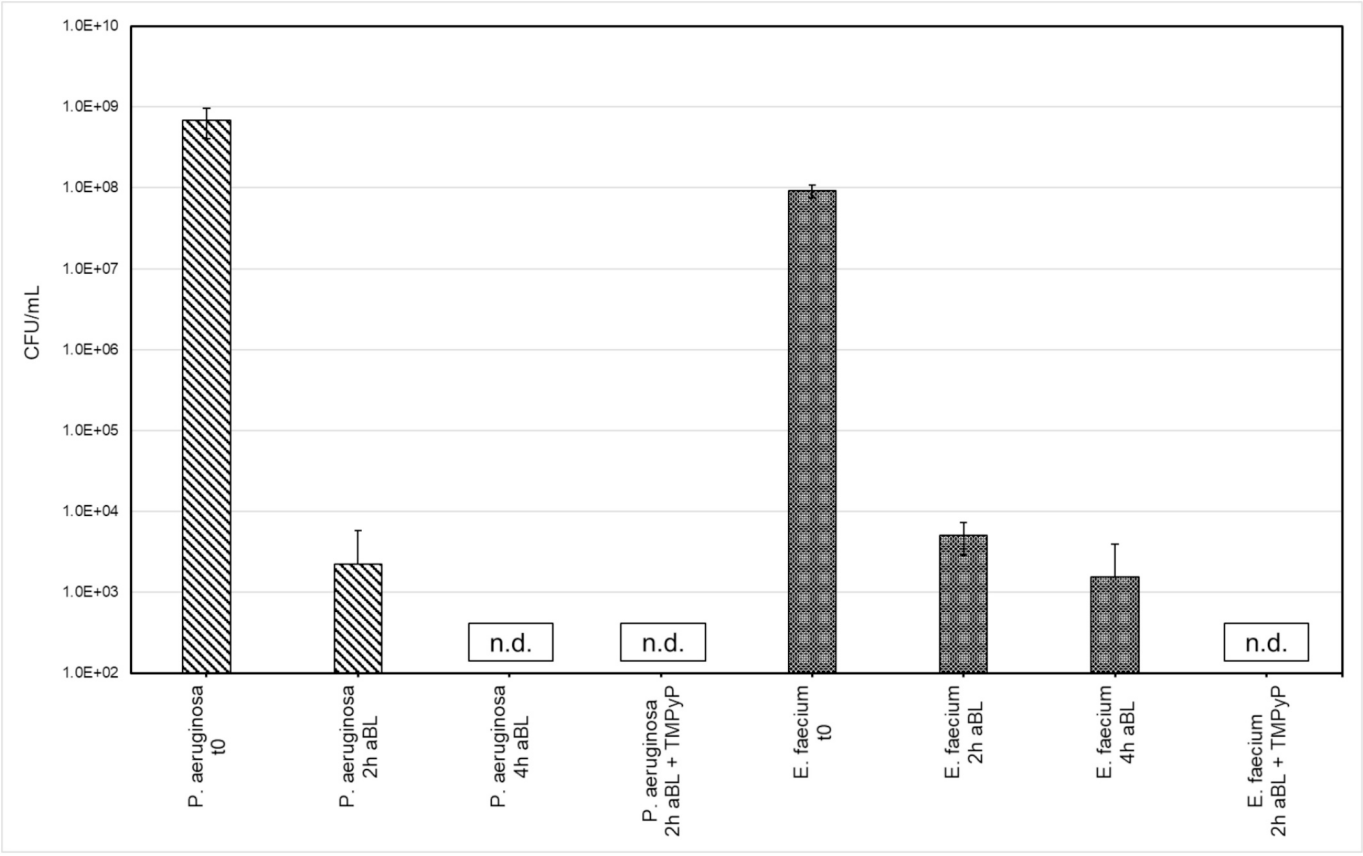

Fig. 2. Logarithmic CFU/mL values, including standard deviations, are shown as light patter bars for *P. aeruginosa* and dark bars for *E. faecium*. Data are presented for untreated initial samples (t_o) and for samples following 2 h aBL, 4 h aBL, and 2 h aBL + TMPyP treatments (n=3). All aBL exposures were conducted using 420 nm LED lamps within a static photoreactor. In case of no colony detection these samples are indicated by n.d.: not detected.

Although CFU numbers only offer an estimation of viability, qPCR let us assess the presence of undamaged genetic material, thereby uncovering possible persistence mechanisms such as VBNC. Notably, the addition of TMPyP significantly enhanced aBL efficacy, especially against *E. faecium*, and may help overcome limitations related to sub-lethal or stress-tolerant bacterial states. These findings emphasize the necessity to carefully choose the analytical methodology in order to properly assess and optimize new disinfection procedures.

3.2. Identification of specific ROS responsible for the degradation of ARGs and FPB

Two aBL-treated groups (aBL, aBL/TMPyP) were analyzed for the efficacy of inactivation of the *A. baumannii*, and degradation of three selected genes (*erm*B, 16S rRNA, and bla_{TEM}) in this region. *A. baumannii* was selected because it is an ESKAPE pathogen and a WHO critical-priority organism (carbapenem-resistant lineages), is frequently detected in municipal wastewater and hospital effluents. 16S rRNA provides a broad proxy for total bacterial DNA, *erm*B is a prevalent and often mobile macrolide resistance marker in wastewater, and bla_{TEM} represents a clinically important β-lactamase gene commonly found in WWTP ecosystems. Notably, our previous study employed a substantially broader suite of taxa and ARGs to establish the overall efficacy of aBL/aBL + photosensitizer; the present work builds on that foundation to resolve which ROS dominate under wastewater conditions and how strongly they affect representative genetic targets. The samples were collected from the influent of the WWTP at KIT. The static aBL photoreactor used in these experiments is illustrated in Fig. S3.

aBL combined with TMPyP appeared to be the optimal aBL tested for the killing of *A. baumannii* and the eradication of the three genes targeted (as presented in Fig. 3). The individual cell equivalents obtained from qPCR for treatments with ROS scavengers were compared to those without scavengers. The results are presented as $\log_{10}$ fold changes, as shown in Fig. 3. A value around 0 indicates that the addition of a scavenger had little to no effect on gene abundance, suggesting minimal interference with ROS activity. Positive $\log_{10}$ values reflect an increase in gene abundance relative to the treatment alone, indicating that the scavenger reduced the efficacy of photoinactivation, likely by quenching ROS. Higher values, therefore, suggest greater ROS involvement in the treatment effect. Notably, the aBL + TMPyP treatment group showed the most substantial decline in gene copy numbers, with a particularly stronger decrease in 16S rRNA gene abundance (as shown in Table S3) and this effect was markedly diminished upon the addition of some ROS scavengers. This comes from that this combination was apparently most efficient in generating ROS, which we discussed above. The comparative analysis further demonstrated that the effectiveness of each treatment is directly influenced by the type and concentration of ROS generated, as well as by the susceptibility of specific bacterial strains and genetic targets. Particularly, $^1O_2$ and H_2O_2 have been identified as the major species contributing to the bacterial and gene degredation in the aBL + TMPyP regimen. In line with this, the addition of L-histidine and Na_2SO_3 (as quencher of $^1O_2$ and H_2O_2, respectively) resulted in a quantifiable reduction of the antimicrobial effect: for $^1O_2$ scavenging, gene copy numbers increased by approximately 2 $\log_{10}$ units for all investigated targets. Similarly, quenching H_2O_2 resulted in approximately 2 $\log_{10}$ increase for *sec*E, 16S, and around 1 $\log_{10}$ increase for bla_{TEM}, and a more pronounced 3.2 $\log_{10}$ increase for *erm*B after 4 h of treatment. Such uniform pattern of all the genes quantified confirms the key role played by $^1O_2$ and H_2O_2 as main ROS inducing gene degradation and bacterial inactivation under aBL + TMPyP treatment

Table 1
The cell equivalents/100 mL are presented as mean values with standard deviation, along with the resulting log_{10} reductions, which are calculated relative to the average initial concentration at t_0 following 2 h aBL, 4 h aBL, and 2 h aBL + TMPyP treatments. The mean values of the cell equivalents/100 mL are calculated for t_0 ($n = 9$) and for the individual irradiation conditions ($n = 3$) for all four qPCR targets. *ecf*X and *23S* represent taxonomic gene markers for *P. aeruginosa* and *E. faecium*, respectively, while bla_{VIM} and *van*A denote their corresponding antibiotic resistance genes. Positive log_{10} values indicate a reduction in gene copy number, whereas negative values reflect no reduction. Larger absolute values correspond to greater changes in concentration. The log_{10} reductions of 2 h aBL + TMPyP are highlighted in bold to compare *P. aeruginosa* and *E. faecium*.

Sample	Cell equivalents/100 mL	Log_{10} reduction
*ecf*X (*P. aeruginosa*), reference t_0	$1.23 \times 10^{10} \pm 2.04 \times 10^9$	−0.47 (no reduction)
*ecf*X (*P. aeruginosa*), 2 h aBL	$3.64 \times 10^{10} \pm 4.32 \times 10^9$	
*ecf*X (*P. aeruginosa*), 4 h aBL	$8.94 \times 10^9 \pm 6.47 \times 10^8$	0.14
ecfX (*P. aeruginosa*), 2 h aBL + TMPyP	**$8.33 \times 10^8 \pm 9.03 \times 10^7$**	**1.17**
bla_{VIM} (*P. aeruginosa*), reference t_0	$4.46 \times 10^{10} \pm 6.14 \times 10^9$	−0.32 (no reduction)
bla_{VIM} (*P. aeruginosa*), 2 h aBL	$9.37 \times 10^{10} \pm 3.53 \times 10^9$	
bla_{VIM} (*P. aeruginosa*), 4 h aBL	$1.50 \times 10^{10} \pm 7.73 \times 10^9$	0.47
bla_{VIM} (*P. aeruginosa*), 2 h aBL + TMPyP	**$1.69 \times 10^9 \pm 1.38 \times 10^9$**	**1.42**
23S (*E. faecium*), reference t_0	$2.67 \times 10^{10} \pm 3.00 \times 10^9$	−0.17 (no reduction)
23S (*E. faecium*), 2 h aBL	$4.00 \times 10^{10} \pm 2.38 \times 10^9$	
23S (*E. faecium*), 4 h aBL	$5.21 \times 10^9 \pm 7.63 \times 10^7$	0.71
23S (*E. faecium*), 2 h aBL + TMPyP	**$6.58 \times 10^4 \pm 4.19 \times 10^3$**	**5.61**
*van*A (*E. faecium*), reference t_0	$3.38 \times 10^{11} \pm 8.21 \times 10^{10}$	−0.19 (no reduction)
*van*A (*E. faecium*), 2 h aBL	$5.26 \times 10^{11} \pm 1.09 \times 10^{11}$	
*van*A (*E. faecium*), 4 h aBL	$5.84 \times 10^{10} \pm 7.90 \times 10^9$	0.76
vanA (*E. faecium*), 2 h aBL + TMPyP	**$2.46 \times 10^4 \pm 2.41 \times 10^3$**	**7.14**

(Fig. 3 (B)).

The relatively limited efficacy of aBL alone suggests that, while partially effective, this treatment may require optimization or combination with other agents to achieve maximal inactivation of bacteria and ARGs. This is also confirmed by the scavenger assay, since ROS inhibition in these treatments resulted in less than one log_{10} unit of higher gene copy numbers for all the targets detected (Fig. 3(A)). As we did not directly quantify ROS, we do not draw conclusions about ROS yields. We interpret the small scavenger effects as evidence that, under our conditions, ROS made only a limited but detectable contribution to the measured molecular endpoint. We infer that ROS were not the principal drivers of gene degradation, or that their effects fell below our assay's sensitivity. These observations motivate tests that amplify ROS pathways.

The measured attenuation of the aBL antimicrobial effect after removing ROS further verifies the criticality of ROS in aBL disinfection mechanism. These data highlight the importance of selecting optimized photosensitizers for ROS generation, if treatment efficacy is to be enhanced, especially for decentralized wastewater disinfection applications. Indeed, TMPyP is a very efficient photosensitizer in this respect but more specific derivatives or even a more potent agent might be subject to future studies, including better definition of the irradiation

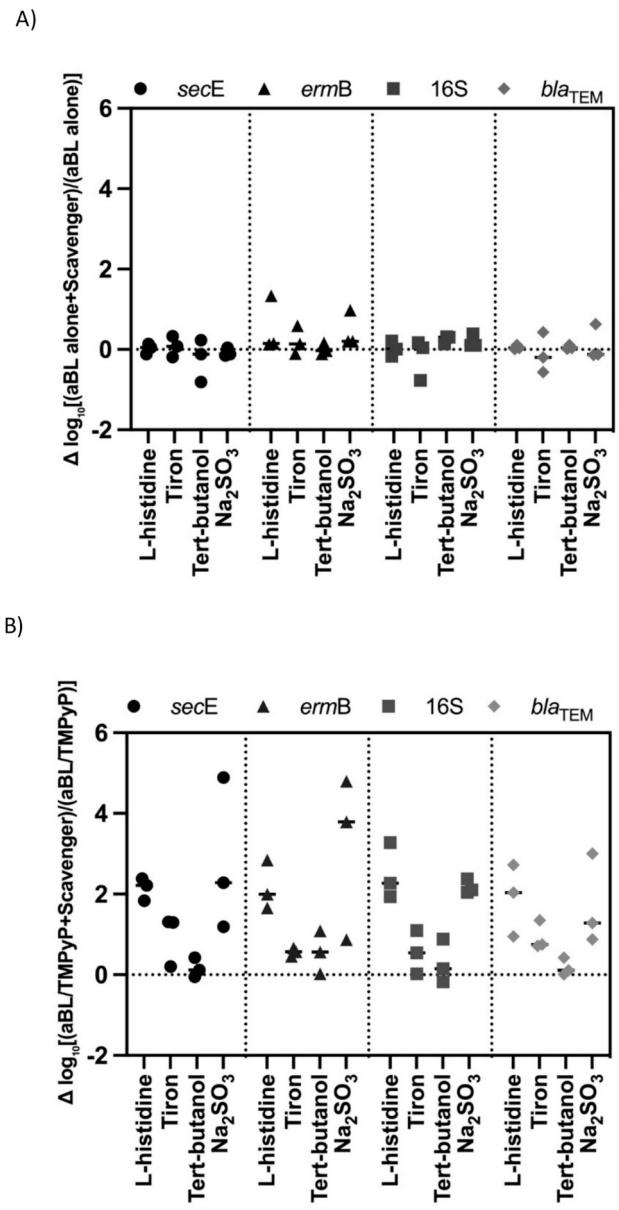

Fig. 3. The plots show the relative abundance of bacterial genes after treatment with different ROS scavengers (L-histidine, Tiron, Tert-butanol, Na_2SO_3) combined with treatments either (A) aBL alone or (B) the photosensitizer TMPyP (n=3). The y-axis indicates the log_{10}-transformed ratio of gene abundance in treated samples (treatments + scavenger) relative to control (treatments) after 4 h irradiation time, measured in cell equivalents per 100 mL. Each data point represents a qPCR-based quantification of one of four bacterial gene targets: *sec*E, *erm*B, 16S rRNA gene, and bla_{TEM}. Dotted vertical lines separate different scavenger groups, and the same scavenger order is used across both panels. Mean value for each group are indicated by horizontal lines.

conditions and potential synergism with other treatments. In addition, more deep mechanisms are required to understand how the individual ROS interacts with bacteria cells and ARGs at the molecular level. These findings will be critical to guide the rational design and application of future-generation light-activated antimicrobial strategies.

Four scavengers (tert-butanol, Tiron, L-histidine, Na_2SO_3) were used, as previously described, in order to selectively quench ROS species ($OH^•$, $O_2^{•-}$, $^1O_2$, and H_2O_2, respectively). This method facilitated the evaluation of the involvement of ROS in different treatment protocols. To assess the degradation kinetics of bacterial gene targets during different aBL treatment conditions, with or without the addition of ROS

scavengers, a pseudo-first-order kinetic model was applied. Quantification was based on changes in 16S rRNA cell equivalents (Table S3), comparing initial concentration (C_0) to those at time t (240 mins, C_t). Mean values from three independent trials were calculated and used for evaluation and comparison. It is evident that when aBL combined with TMPyP was applied, the corresponding rate constant (*k*) significantly decreased from 0.03 min^{-1} in the control experiment (without scavengers) to 0.006 min^{-1} and 0.009 min^{-1} in the presence of L-histidine and Na_2SO_3, respectively (as shown in Fig. 4 (B)). These results provide evidence that $^1O_2$ and H_2O_2 made the dominant contributions to the degradation of bacteria in this system. Calculated relative contributions (RC) of each ROS in aBL + TMPyP were the following: $^1O_2$ (78 %) > H_2O_2 (68 %) > $O_2^{\bullet-}$ (17 %) > $OH^\bullet$ (9 %). For aBL lone (As shown in Fig. 4 (A)), ROS played a less significant role in bacterial inactivation, as indicated by minimal changes in the degradation rate constant after the addition of specific scavengers. In the case of aBL-alone treatment, $^1O_2$ was the least useful ROS during bacterial inactivation process. On the contrary, contribution rates in $OH^\bullet$, $O_2^{\bullet-}$, and H_2O_2 demonstrated substantially higher relative contributions. Results suggest that while aBL on its own generates multiple ROS, their overall bactericidal impact is limited without an external photosensitizer. The presence of TMPyP is the major determinant that tips the balance toward ROS species, namely $^1O_2$ and H_2O_2, which are relevant for efficient inactivation of bacteria.

These results indicate that the major ROS for bacteria inactivation are quite different, depending on the treatment composition. In particular, $^1O_2$ and H_2O_2 were found to be the most abundant ROS involved in the bactericidal action with the combination of aBL and TMPyP. Furthermore, in the case of aBL applied without specific substances, $OH^\bullet$, $O_2^{\bullet-}$, and H_2O_2 played an important role in bacterial inactivation, whereas $^1O_2$ had the lowest effect. These findings emphasize the need to optimize aBL based disinfection for the ROS differentially produced under different treatment circumstances. Strategic optimization, e.g., choosing the suitable photosensitizers and ROS enhancers, and maintaining small local variations in the wastewater microbial communities are needed to maximize the bacteria inactivation and ARGs degradation.

3.3. Quantification of ROS-responsive regulatory genes

RT-qPCR showed the different gene expression responses to various aBL treatments. The samples were collected from the influent of the WWTP at KIT. In the Table 2, we show the $2^{-\Delta\Delta Ct}$-derived expression fold changes of five core genes (i.e., *rec*A, *sod*A, *omp*F, *oxy*R, and *tol*C) to three treatment options (aBL alone, aBL + H_2O_2 and aBL + TMPyP). These treatment conditions were consistent with those used in our previous study (Cong et al., 2025).

All treatments resulted in significantly increased expression of *sod*A,

Table 2
Quantitative analysis of relative gene expression in wastewater from WWTP influent treated with aBL under three conditions: aBL alone, aBL+H_2O_2, aBL+TMPyP. Expression of five target genes (*rec*A, *sod*A, *omp*F, *oxy*R, *tol*C) was measured via RT-qPCR and calculated using the $2^{-\Delta\Delta Ct}$ method, normalized to 16S rRNA. Results are expressed as x-fold change relative to the untreated control, which is set to a value of 1. Data represent the mean ± standard deviation from four independent biological replicates (n=4). Statistical significance compared to the control was assessed using the Mann-Whitney *U* test; p values < 0.1 were considered significant and are indicated in bold.

Normalized to 16S rRNA expression				
		x-fold change	st.dev	p-value
***rec*A**	aBL alone	0.96	0.63	0.6
	aBL+H_2O_2	0.71	0.28	0.3429
	aBL+TMPyP	2.5	2.39	–
***sod*A**	aBL alone	2.48	2.14	0.8857
	aBL+H_2O_2	1.34	1.37	0.4857
	aBL+TMPyP	0.72	0.49	0.4857
***omp*F**	aBL alone	0.13	0.03	**0.0571**
	aBL+H_2O_2	0.21	0.25	**0.0571**
	aBL+TMPyP	1.12	0.68	0.8857
***oxy*R**	aBL alone	2.65	2.46	0.6857
	aBL+H_2O_2	2.82	4	0.8857
	aBL+TMPyP	3.11	1.81	0.2
***tol*C**	aBL alone	1.38	0.41	–
	aBL+H_2O_2	2.57	3.39	–
	aBL+TMPyP	4.29	2.93	0.3429

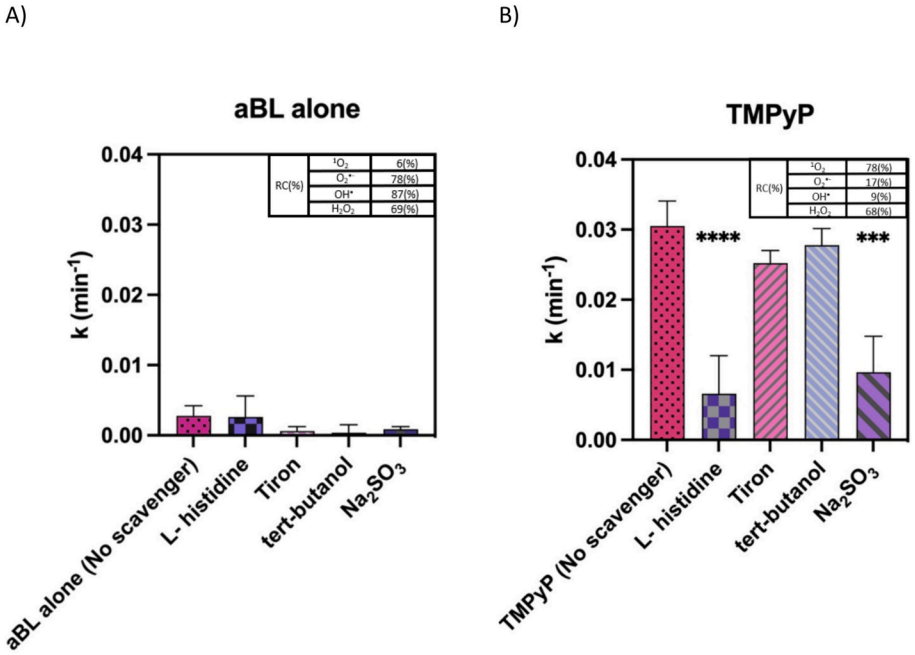

Fig. 4. Comparative analysis of the degradation kinetics (*k*/min) of bacterial cells under (A) aBL alone and (B) aBL+TMPyP in the presence and absence of specific ROS scavengers. Each treatment was evaluated with four scavengers: L-histidine (targeting $^1O_2$), Tiron ($O_2^{\bullet-}$), tert-butanol ($OH^\bullet$), and Na_2SO_3 (H_2O_2). Bars represent the mean degradation rate constants (k) ± standard deviation (n=3), and statistical significance is indicated as $p \leq 0.0001$(****), $p \leq 0.001$ (***). Insets show the calculated relative contributions (RC%) of each ROS to bacterial inactivation for the respective treatment.

*rec*A, *oxy*R and *tol*C, most notably by aBL combined with TMPyP, and a decrease in *omp*F. Excessive ROS can activate the processes of detoxification as well as culminate in the SOS response in bacterial cells. The gene product of *sod*A enzyme, which is a key enzyme for detoxification of oxidative stress, was significantly up-regulated under aBL treatment alone (>2-fold in the present study), being indicative of the strong oxidative stress response. This observation is supported by ROS scavenging assays and detected significant generation of $O_2^{\bullet-}$ in the existence of aBL. Also, the expression of *rec*A, which is a key regulator in the SOS response, was highly induced (>2-fold) when aBL was added to TMPyP, implying possible genotoxic damage and the induction of the subsequent DNA repair system. *Oxy*R, which is also involved in H_2O_2 detoxification, was the most strongly induced gene (>3-fold) following aBL+TMPyP treatment, emphasising the increased oxidative stress generated by this combined treatment.

Of all the outer membrane protein genes studied, *tol*C, which is associated with efflux pump systems, was significantly upregulated in all aBL-related treatments as compared to control conditions and this change was especially pronounced (> 3-fold) under aBL+TMPyP, indicating increased efflux of toxic metabolites. In contrast, aBL changed the transcriptional expression of *omp*F in all the experiments, indicating that the *omp*F was down the control suggesting protective reduction in the permeability of the membrane that would result in prevention from entry of toxic substances (Bystritskaya et al., 2014).

Such findings emphasize the strong oxidative and genotoxic stress reaction induced by aBL, particularly after combination with a photosensitizer. The observed transcription profiles highlight the crosstalk between oxidative stress and bacterial defense mechanisms. It supports the involvement of ROS through the up-regulation of stress response genes, particularly under aBL plus TMPyP. Specifically, the upregulation of key genes, including those involved in antioxidant defense (*sod*A), DNA repair (*rec*A) and membrane stess response (*tol*C), confirms that aBL-based treatments induce both DNA and membrane damage.

These molecular responses are correlated with the earlier discovery showed by ROS scavenger and gene degradation tests, supporting a conclusion that aBL-based disinfection induced a variety of stress pathways, such as antioxidant defense, DNA repair, and cell membrane adaption mechanisms. Overall, the evidence suggests that aBL treatments trigger a coordinated bacterial response encompassing oxidative detoxification, SOS-mediated DNA repair, and adaptive membrane regulation.

4. Conclusion and perspectives

This work proves aBL, especially with the presence of the photosensitizer, is an efficiently emerging approach for inactivation of ARB and ARGs in wastewater. The relative values obtained from CFU enumeration and qPCR indicate that it was necessary to use culture-dependent and molecular methods in parallel to better examine the effectiveness of disinfection strategies, especially for organisms that may be able to enter into a VBNC state. Notably, understanding the mechanisms behind inactivation strategies requires insights into physiological and genetic responses that cultivation alone cannot provide. Therefore, in this study, molecular analyses, including gene degradation and expression profiling, were employed to elucidate the mechanisms underlying the antimicrobial effects of the innovative aBL technology.

Compared with other aBL treatments, aBL+TMPyP yielded the highest inactivation efficiency, mediated by ROS production, especially $^1O_2$, which was the primary ROS for gene and cell degradation. Upregulation of oxidative stress response genes (*oxy*R, *sod*A, *rec*A, and *tol*C) and downregulation of *omp*F which were confirmed by RT-qPCR, signified that the bacteria had successfully adapted to the ROS-induced damage. Collectively, our results establish a mechanistic basis for ROS-mediated disinfection and demonstrate the feasibility of aBL as a decentralized wastewater treatment option. The technology can support pilot-scale installation and on-site deployment. The approach offers a low-risk, mercury-free alternative to conventional UV systems, which is particularly suitable for high-risk effluents at AMR hotspots. The findings provide guidance for reactor design and operating conditions. Future work should optimize light parameters, photosensitizer selection, and combinatory treatments. These optimizations will increase efficacy and enable real-world application.

CRediT authorship contribution statement

Xiaoyu Cong: Visualization, Validation, Software, Methodology, Data curation, Writing – original draft. **Jasna Hillert:** Visualization, Methodology, Investigation, Data curation. **Peter Krolla:** Visualization, Software, Methodology, Investigation. **Thomas Schwartz:** Validation, Supervision, Project administration, Funding acquisition, Conceptualization, Writing – review & editing.

Declaration of competing interest

The authors declare that they have no known competing financial interests or personal relationships that could have appeared to influence the work reported in this paper.

Acknowledgement

We thank the JPI-AMR initiative and the German BMBF-DLR for financial support within the framework of the HOTMATS project. We also acknowledge the support of KIT, as well as the local wastewater treatment plant operators for providing wastewater and conventionally treated samples. Special thanks go to all project partners involved in the collection and provision of the analyzed samples.

Appendix A. Supplementary data

Supplementary data to this article can be found online at https://doi.org/10.1016/j.scitotenv.2025.180878.

Data availability

Data will be made available on request.

References

Alexander, J., Knopp, G., Dötsch, A., Wieland, A., Schwartz, T., 2016. Ozone treatment of conditioned wastewater selects antibiotic resistance genes, opportunistic bacteria, and induce strong population shifts. Sci. Total Environ. 559, 103–111.

Amarasiri, M., Sano, D., Suzuki, S., 2020. Understanding human health risks caused by antibiotic resistant bacteria (ARB) and antibiotic resistance genes (ARG) in water environments: current knowledge and questions to be answered. Crit. Rev. Environ. Sci. Technol. 50 (19), 2016–2059.

Bang, Y.J., Lee, Z.W., Kim, D., Jo, I., Ha, N.C., Choi, S.H., 2016. OxyR2 functions as a three-state redox switch to tightly regulate production of Prx2, a peroxiredoxin of Vibrio vulnificus. J. Biol. Chem. 291 (31), 16038–16047.

Baptista, M.S., Cadet, J., Greer, A., Thomas, A.H., 2021. Photosensitization reactions of biomolecules: definition, targets and mechanisms. Photochem. Photobiol. 97 (6), 1456–1483.

Berditsch, M., Jäger, T., Strempel, N., Schwartz, T., Overhage, J., Ulrich, A.S., 2015. Synergistic effect of membrane-active peptides polymyxin B and gramicidin S on multidrug-resistant strains and biofilms of Pseudomonas aeruginosa. Antimicrob. Agents Chemother. 59 (9), 5288–5296.

Bulit, F., Grad, I., Manoil, D., Simon, S., Wataha, J.C., Filieri, A., Bouillaguet, S., 2014. Antimicrobial activity and cytotoxicity of 3 photosensitizers activated with blue light. J Endodont 40 (3), 427–431.

Bustin, S.A., Benes, V., Garson, J.A., Hellemans, J., Huggett, J., Kubista, M., Wittwer, C. T., 2009. The MIQE guidelines: Minimum Information for Publication of quantitative Real-Time PCR Experiments. Clin. Chem. 55 (4), 611–622.

Bystritskaya, E.P., Stenkova, A.M., Portnyagina, O.Y., Rakin, A.V., Rasskazov, V.A., Isaeva, M.P., 2014. Regulation of Yersinia pseudotuberculosis major porin expression in response to antibiotic stress. Mol. Genet. Microbiol. Virol. 29, 63–68.

Chaves, J.C.A., dos Santos, C.G., de Miranda, É.G.A., Junior, J.T.A., Nantes, I.L., 2017. Free-base and metal complexes of 5, 10, 15, 20-Tetrakis (NMethyl Pyridinium L) porphyrin: catalytic and therapeutic properties. In: Phthalocyanines and Some Current Applications. IntechOpen.

Chiang, S.M., Schellhorn, H.E., 2012. Regulators of oxidative stress response genes in Escherichia coli and their functional conservation in bacteria. Arch. Biochem. Biophys. 525 (2), 161–169.
Choudhary, D., Foster, K.R., Uphoff, S., 2024. The master regulator OxyR orchestrates bacterial oxidative stress response genes in space and time. Cell Syst. 15 (11), 1033–1045.
Colwell, R.R., 2000. Viable but nonculturable bacteria: a survival strategy. J. Infect. Chemother. 6, 121–125.
Cong, X., Krolla, P., Khan, U.Z., Savin, M., Schwartz, T., 2023. Antibiotic resistances from slaughterhouse effluents and enhanced antimicrobial blue light technology for wastewater decontamionation. Environ. Sci. Pollut. Res. 30 (50), 109315–109330.
Cong, X., Schwermer, C.U., Krolla, P., Schwartz, T., 2025. Inactivating facultative pathogen bacteria and antibiotic resistance genes in wastewater using blue light irradiation combined with a photosensitizer and hydrogen peroxide. Sci. Total Environ. 974, 179208.
Dąbrowski, J.M., 2017. Reactive oxygen species in photodynamic therapy: mechanisms of their generation and potentiation. In: Advances in Inorganic Chemistry, 70. Academic Press, pp. 343–394.
Ding, D., Wang, B., Zhang, X., Zhang, J., Zhang, H., Liu, X., Yu, Z., 2023. The spread of antibiotic resistance to humans and potential protection strategies. Ecotoxicol. Environ. Saf. 254, 114734.
Ferro, G., Guarino, F., Cicatelli, A., Rizzo, L., 2017. β-lactams resistance gene quantification in an antibiotic resistant Escherichia coli water suspension treated by advanced oxidation with UV/H_2O_2. J. Hazard. Mater. 323, 426–433.
Feuerstein, O., Ginsburg, I., Dayan, E., Veler, D., Weiss, E.I., 2005. Mechanism of visible light phototoxicity on Porphyromonas gingivalis and Fusobacterium nucleatum. Photochem. Photobiol. 81 (5), 1186–1189.
Han, J., Li, W., Yang, Y., Zhang, X., Bao, S., Zhang, X., Leung, K.M.Y., 2024. UV-based advanced oxidation processes for antibiotic resistance control: efficiency, influencing factors, and energy consumption. Engineering 37, 27–39.
Hembach, N., Alexander, J., Hiller, C., Wieland, A., Schwartz, T., 2019. Dissemination prevention of antibiotic resistant and facultative pathogenic bacteria by ultrafiltration and ozone treatment at an urban wastewater treatment plant. Sci. Rep. 9 (1), 12843.
Herigstad, B., Hamilton, M., Heersink, J., 2001. How to optimize the drop plate method for enumerating bacteria. J. Microbiol. Methods 44 (2), 121–129.
Kruszewska-Naczk, B., Grinholc, M., Waleron, K., Bandow, J.E., Rapacka-Zdończyk, A., 2024. Can antimicrobial blue light contribute to resistance development? Genome-wide analysis revealed aBL-protective genes in *Escherichia coli*. Microbiol. Spectrum 12 (1) e02490-23.
Li, W., Zhang, G., 2022. Detection and various environmental factors of antibiotic resistance gene horizontal transfer. Environ. Res. 212, 113267.
Li, S., Ondon, B.S., Ho, S.H., Zhou, Q., Li, F., 2023. Drinking water sources as hotspots of antibiotic-resistant bacteria (ARB) and antibiotic resistance genes (ARGs): occurrence, spread, and mitigation strategies. J. Water Process Eng. 53, 103907.
Livak, K.J., Schmittgen, T.D., 2001. Analysis of relative gene expression data using real-time quantitative PCR and the $2^{-\Delta\Delta CT}$ method. methods 25 (4), 402–408.
Mandal, T.K., 2024. Nanomaterial-enhanced hybrid disinfection: a solution to combat multidrug-resistant bacteria and antibiotic resistance genes in wastewater. Nanomaterials 14 (22), 1847.
Martín-Sómer, M., Pablos, C., Adán, C., van Grieken, R., Marugán, J., 2023. A review on LED technology in water photodisinfection. Sci. Total Environ. 885, 163963.
Méndez-Hurtado, J., López, R., Suárez, D., Menéndez, M.I., 2012. Theoretical study of the oxidation of histidine by singlet oxygen. Chem Eur J 18 (27), 8437–8447.
Ngo, V.N., Truong, T.N.T., Tran, T.T., Nguyen, L.T., Mach, N.B., Vu, V.V., Vu, T.M., 2023. A combination of blue light at 460 nm and H_2O_2 for the safe and effective eradication of *Staphylococcus aureus* in an infected mouse skin abrasion model. Microorganisms 11 (12), 2946.
Ondon, B.S., Li, S., Zhou, Q., Li, F., 2021. Sources of antibiotic resistant bacteria (ARB) and antibiotic resistance genes (ARGs) in the soil: a review of the spreading mechanism and human health risks. Rev. Environ. Contam. Toxicol. 256, 121–153.
O'Neill, J., 2016. Tackling Drug-Resistant Infections Globally: Final Report and Recommendations.
Patel, R., Uhl, J.R., Kohner, P., Hopkins, M.K., Cockerill 3rd, F.R., 1997. Multiplex PCR detection of *van*A, *van*B, *van*C-1, and *van*C-2/3 genes in enterococci. J. Clin. Microbiol. 35 (3), 703–707.
Pfaffl, M.W., 2001. A new mathematical model for relative quantification in real-time RT–PCR. Nucleic Acids Res. 29 (9), e45.
Piechowski, M.V., Thelen, M.A., Hoigné, J., Bühler, R.E., 1992. Tert-Butanol as an OH-scavenger in the pulse radiolysis of oxygenated aqueous systems. Ber. Bunsenges. Phys. Chem. 96 (10), 1448–1454.
Qi, W., Jonker, M.J., de Leeuw, W., Brul, S., Ter Kuile, B.H., 2023. Reactive oxygen species accelerate de novo acquisition of antibiotic resistance in *E. coli*. Iscience 26 (12).
Rapacka-Zdonczyk, A., Wozniak, A., Kruszewska, B., Waleron, K., Grinholc, M., 2021. Can gram-negative bacteria develop resistance to antimicrobial blue light treatment? Int. J. Mol. Sci. 22 (21), 11579.
Sanchez-Alberola, N., Campoy, S., Barbé, J., Erill, I., 2012. Analysis of the SOS response of Vibrio and other bacteria with multiple chromosomes. BMC Genomics 13, 1–12.
Schacksen, P.S., Macêdo, W.V., Rellegadla, S., Vergeynst, L., Nielsen, J.L., 2025. Dynamics of nitrogen-transforming microbial populations in wastewater treatment during recirculation of hydrothermal liquefaction process-water. Water Res. 276, 123254.
Shao, S., Hu, Y., Cheng, J., Chen, Y., 2018. Research progress on distribution, migration, transformation of antibiotics and antibiotic resistance genes (ARGs) in aquatic environment. Crit. Rev. Biotechnol. 38 (8), 1195–1208.
Smith, C.J., Osborn, A.M., 2009. Advantages and limitations of quantitative PCR (Q-PCR)-based approaches in microbial ecology. FEMS Microbiol. Ecol. 67 (1), 6–20.
Sorn, S., Sabar, M.A., Hara-Yamamura, H., Matsuura, N., Watanabe, T., Yamamoto-Ikemoto, R., Honda, R., 2023. Unravelling Antibiotic resistance mechanisms in wastewater treatment: transcription of args and the role of stress conditions.
Taiwo, F.A., 2008. Mechanism of tiron as scavenger of superoxide ions and free electrons. J. Spectrosc. 22 (6), 491–498.
Tang, K.W.K., Millar, B.C., Moore, J.E., 2023. Antimicrobial resistance (AMR). Br. J. Biomed. Sci. 80, 11387.
Taylor, J.C., Gu Liu, C., Chang, J.D., Thompson, B.E., Maresso, A.W., 2024. Gene discovery from microbial gene libraries I: protection against reactive oxygen species-driven DNA damage. Microbiol. Spectr. 12 (11), e00365-24.
Truong, H.B., Huy, B.T., Ray, S.K., Lee, Y.I., Cho, J., Hur, J., 2020. H_2O_2-assisted photocatalysis for removal of natural organic matter using nanosheet C_3N_4-WO_3 composite under visible light and the hybrid system with ultrafiltration. Chem. Eng. J. 399, 125733.
Wang, J., Chen, X., 2022. Removal of antibiotic resistance genes (ARGs) in various wastewater treatment processes: an overview. Crit. Rev. Environ. Sci. Technol. 52 (4), 571–630.
Wang, Y., Li, W., Irini, A., 2013. A novel and quick method to avoid H_2O_2 interference on COD measurement in Fenton system by Na_2SO_3 reduction and O_2 oxidation. Water Sci. Technol. 68 (7), 1529–1535.
Wang, Y., Ferrer-Espada, R., Baglo, Y., Gu, Y., Dai, T., 2019. Antimicrobial blue light inactivation of Neisseria gonorrhoeae: roles of wavelength, endogenous photosensitizer, oxygen, and reactive oxygen species. Lasers Surg. Med. 51 (9), 815–823.
Wang, Y., Yang, J., Zhao, R., Zhang, S., Guo, J., Wang, J., 2024. Nonantibiotic pharmaceuticals exhibit antibacterial activity and enhance bacterial evolution toward antibiotic resistance. ACS ES&T Water 4 (4), 1701–1710.